Platelet enrichment from whole blood in a clog-free microfluidic radial pillar device (RAPID)

Ninad Mehendale,[a] Oshin sharma,[a] Claudy D'Costa,[a] and Debjani Paul[a]

[a] *Indian Institute of Technology Bombay*

We report platelet enrichment from whole blood in a novel radial pillar device (RAPID) recently developed by us. Isolation of platelets from whole blood is required for understanding of clotting and the diagnosis of various diseases (e.g. dengue, thrombocytopenia, etc.). Size-based separation of platelets from a background of other blood cells in passive microfluidic devices is extremely challenging as the red blood cells are highly deformable and can pass through gaps much smaller than their size. Pillar-based microfluidic devices get clogged very soon, or lack the selectivity required for size-based separation. RAPID combines the advantages of dead-end and cross-flow pillar devices. Self-unclogging is achieved in RAPID by continuous removal of RBCs through secondary cross flows. Our device is most suitable for enriching platelets from whole blood at low flow rates, thus avoiding platelet activation. We report clog-free operation of the device using whole blood for more than 8 hours, which is an extremely challenging feat for pillar-based devices.

1 Introduction

Platelets, also known as thrombocytes, play an important role in clotting of blood[1]. Many diseases, such as, dengue, thrombocytosis, jaundice, rheumatoid arthritis, vitamin B-12 deficiency, pancreatitis, thrombocytopenia, etc. are associated with an abnormal platelet count[2–4]. In healthy people, the ratio of platelets to red blood cells (RBCs) is about 1:20, which makes counting of platelets directly from whole blood challenging. Platelet count can be made easier and more accurate if blood is enriched with platelets by removing most of the RBCs[5,6]. Since, there are approximately 20 RBCs for every platelet in whole blood, an enrichment factor of 20 or above is within acceptable limits[7].There are other benefits of platelet enrichment besides counting. The ability to study the platelets enriched from a heterogeneous mixture of blood is one of the prerequisites for many diagnostic studies associated with clotting[8,9]. There is also an increase in the platelet storage lifespan if platelets are isolated from other blood cells[10].

Separation of platelets from whole blood requires a lot of preprocessing[11,12]. The traditional centrifugation method of blood cell separation is based on density and hence it cannot separate white blood cells (WBCs) and platelets effectively in a single step[13–15]. A secondary separation of the buffy coat containing WBCs and platelets needs to be performed[12,16]. Hence, there is a need for a simplified one-step platelet separation process on a microfluidic chip. Blood cell fractionation has been demonstrated in microfluidic platforms using various methods, such as, inertial focusing[5,17–20], pinched flow fractionation(PFF)[21–24], hydrodynamic lift[25], deterministic lateral displacement (DLD)[26–30], hydrophoretic filtration[31], dead-end pillar filtration[32,33], cross-flow filtration[24,32,34–36], transient cellular adhesion[37–40] etc. These devices are focused on the separation of WBCs and RBCs, or isolation of circulating tumor cells (CTCs) from blood, and very few focus on platelet separation.

There are some recent reports on microfluidic devices which are capable of specifically enriching platelets from blood[11,12,16,41]. Pommer, *et al.*[12] demonstrated dielectrophoretic separation of platelets in a complex two-level microfluidic device. Chen[42] and Nam[11] performed platelet separation using surface acoustic waves (SAW). All of these methods require integrated transducers and high voltages for platelet separation. Subsequently, Nam and others reported a passive platelet separator based on elasto-inertial effects[41]. A major advantage of this work is the use of a passive technique, while maintaining high separation parameters. But this method requires off-chip sample preprocessing, such as, mixing of dilute blood with a non-Newtonian liquid, prior to separation in the microfluidic chip. It is also necessary to replace the non-Newtonian fluid with a Newtonian buffer after separation and prior to counting the blood cells in a flow cytometer. Xia *et al.*[43] achieved 1000X reduction of WBCs from a platelet-rich plasma using controlled incremental filtration. Their results were not obtained with whole blood, but relied on off-chip preparation of platelet-rich plasma. A single-step platelet separation technique (iPC or interfacial platelet cytometry)[44] using an affinity-based approach was reported. The problem with affinitybased methods is that the separated platelets remain adhered to the device surface and any further testing needs to be done on the same chip itself[45].

Size-based separation of platelets from blood in a single step has been attempted in a dead-end pillar filter[46]. Smaller platelets (2-3 μm) are expected to pass through the gap between the pillars, while larger WBCs (10-30 μm) and RBCs (6-8 μm) are expected to be blocked. However, healthy RBCs are biconcave in shape (6-8 μm in diameter and 2-3 μm thick) and very deformable. At higher flow rates, RBCs can squeeze through pillar gaps much smaller than their size (supplementary video SV1). To address this problem, the size cut-off needs to be set to ≤ 1μm. It is very difficult to fabricate such small pillar gaps with high accuracy. Even when these structures can be fabricated, the pillars get clogged by the bigger cells during the experiment[32]. Some remedial measures taken to free the clogged cells from dead-end pillars are making the pillar gaps ratchet-shaped[47] and oscillating the fluid flow. Cross-flow filters[36] were specifically designed to avoid clogging. But the majority of the platelets remain in the main channel along with other blood cells. The large footprint of cross-flow devices also leads to sample loss[32].

Recently we reported on a passive radial pillar device (RAPID)[48] that combines the selectivity of dead-end filters with the clog-free operation of cross-flow devices. The device has a central inlet and several rows of concentric pillars. The successive rows of pillars are shifted by a pre-determined angle to impart a self-unclogging feature to the device without needing any reverse flow. RAPID starts operating like a dead-end filter and becomes a cross-flow filter at the onset of clogging. Previously we demonstrated continuous high-throughput (3ml/min) separation of 1 μm polystyrene beads from a background of 7 μm beads in RAPID. Here we report ~ 50X platelet enrichment from both 20X dilute and whole blood in RAPID without any offchip pre-processing or post-processing of samples. We also report clogging-free operation of the device for 8 hours with whole blood under gravity-driven flow.

2 Materials and methods

2.1 Equipment and chemicals

SU-8 2005 and its developer were obtained from MicroChem Corporation (Westborough, USA). Sylgard 184 (PDMS) was purchased from Dow Corning Corporation (Michigan, USA). Common chemicals, such as, ethanol, isopropyl alcohol, sodium hypochlorite, etc. were obtained from Thomas Baker (Mumbai, India) and used without further purification. Normal saline (0.9% NaCl) was bought locally. 60mm x 24 mm glass cover slips (No. 1) were bought from Blue Star, Mumbai, India. Microfluidic connectors (barb-to-barb WW-30626-48 and luer-to-barb WW30800-06) from Cole Parmer (Mumbai, India) were used, while 1.5 mm diameter Tygon tubing (formulation 2375) was used for chip-to-syringe connections. We used 1 ml plastic syringes from Becton-Dickinson (Mumbai, India). BD vacutainer tubes coated with K2-EDTA were bought from Fisher scientific, USA, for storing blood samples.

Spin coating of photoresist was carried out on model WS400BZ from Laurell Technologies Corporation (PA, USA), and UV exposure was done in a MJB4 mask aligner from Karl Suss. The height of the pillars was measured using an Ambios XP2 profilometer. PDMS-glass bonding was performed using a Harrick plasma cleaner (PDC 32G). A syringe pump (model 111, Cole Parmer) was used to control the blood flow. A vibrator motor (PNN7RB55PW2) was bought locally and attached to the tubes carrying blood. Platelet counts were performed using a hematology analyzer (Sysmax XS-800i). Images of the device were acquired using a Nikon Eclipse Ti inverted microscope fitted with a 40X (1.3 NA) objective.

2.2 Device details

The figure 1(A) shows the schematic diagram of RAPID. It comprises of a central inlet, a single RBC outlet and two platelet outlets. A highlighted sector of the device schematic 1(B) explains the device operation. The pillars are arranged in concentric circles in three zones, each zone having 9 rows of pillars. The innermost zone (around the inlet) stops WBCs and cell aggregates from entering the device. The middle zone (angular displacement or AD zone) prevents sagging of the device and helps to generate a cross-flow. It also houses the RBC outlet. The outermost zone captures the RBCs and lets the platelets pass through to the platelet outlets. There are two key differences in the pillar arrangements of the capture zones (i.e. WBC and RBC captures zones) and the AD zone. First, there is no angular displacement between consecutive rows of pillars in the WBC capture zone. However, the consecutive rows of pillars in the AD zone are shifted by a predetermined angle of 7^o. This sets up a self-circulating cross flow in the AD zone, in addition to the radial flow, as depicted in the schematic of 1(B). Second, the pillar gap is kept constant in the capture zones by progressively increasing the pillar diameters. On the other hand, both the pillar gap and the diameter increase progressively in the AD zone.

The WBC capture zone has 90 pillars in each row, with pillar diameters ranging from 43 μm (row 1) to 60 μm (row 9). This zone captures WBCs and cell aggregates using a pillar gap of 5 μm. AD zone has pillar gaps varying from 5 μm to 10 μm over 9 rows, increasing by 4% at each row. It has 60 pillars in every row, with pillar size ranging from 80 μm (row 1) to 200 μm (row 9). The RBC capture zone has pillar gaps of 2 μm. This has 700 pillars per row, with pillar sizes ranging from 24 μm (row 1) to 26 μm (row 9). The height of the device is 5 μm. Figure 1 (C) shows the profilometry results confirming the height of the device. The inset in figure 1 (D) shows a photo of the fabricated chip with the footprint of 6 mm.

2.3 Device fabrication

RAPID was fabricated using PDMS by standard soft lithography procedure in the IIT Bombay Nanofabrication Facility. A 2-inch

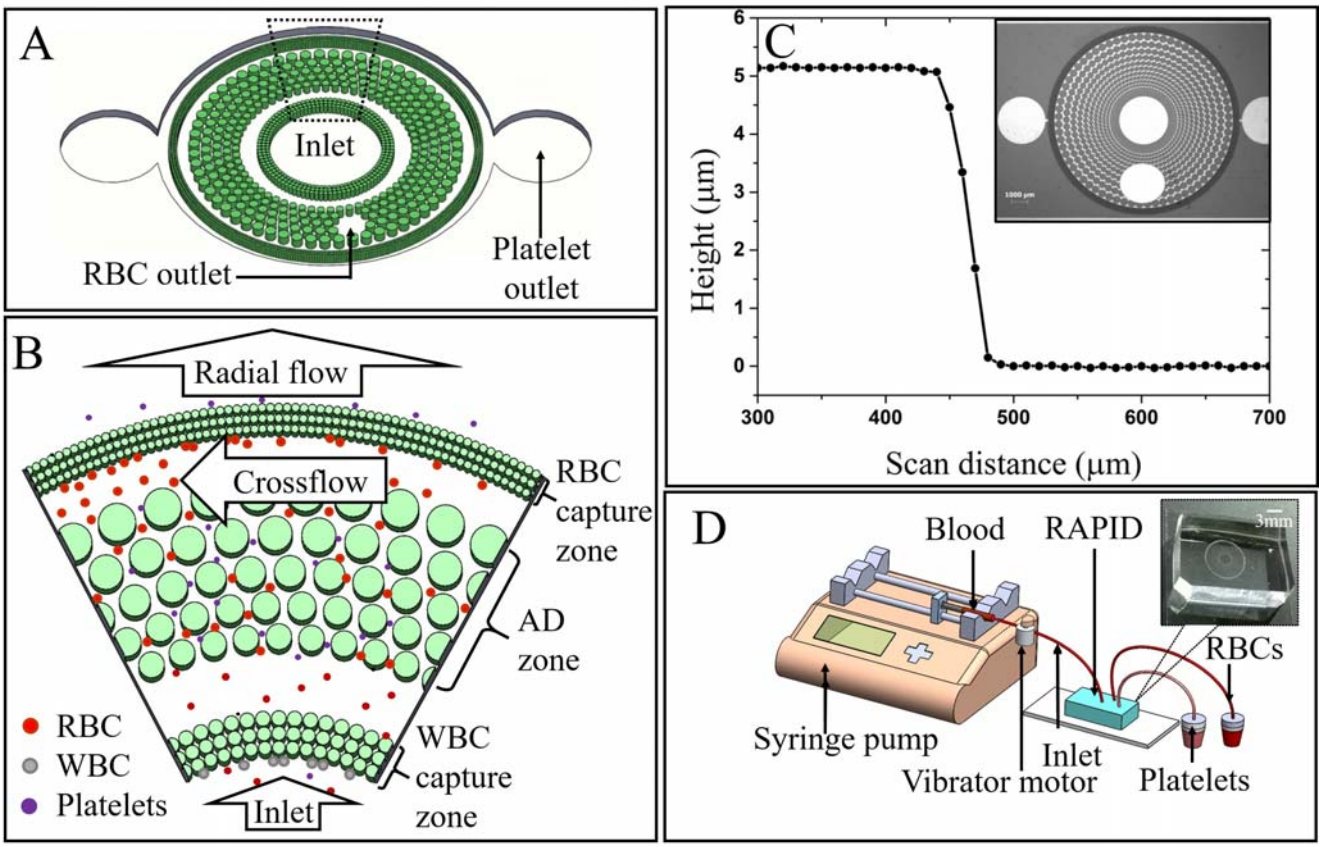

Fig. 1 (A) The schematic diagram of RAPID shows a central inlet, a single RBC outlet and two platelet outlets. The two outlets in the periphery of the device collect the enriched platelet solution, and an outlet in the middle of the device collects the RBCs. (B) A sector of the device schematic is highlighted to explain the device operation. Blood is loaded in the chip through the central inlet and it passes through pillars arranged in concentric circles. The pillars are divided into three zones with progressively varying pillar gaps to separate cells according to their size and deformability. The pillars in the zone adjacent to the inlet prevent cell aggregates and WBCs from entering the device, while allowing the RBCs and the platelets to go through. The successive rows of pillars in the next zone (angular displacement or AD zone) are displaced by a pre-determined angle. The pillars in this zone also prevent the device from sagging. The RBCs are finally stopped by the pillars in the outermost zone (i.e. RBC capture zone) and are carried away by the cross-flow to the RBC outlet. The platelets continue to move out radially and are collected from the two platelet outlets. (C) Profilometry data confirms the device height to be 5μm. The inset shows a microscope image of the fabricated device. The scale bar is 1mm. The inset shows a photo of the fabricated chip. (D) The schematic diagram of the experimental set-up shows a syringe pump, a vibrator motor attached to the inlet tubing, the RAPID chip and two separate Eppendorf tubes for collecting the enriched platelet solution and the RBCs. The inset shows an image of the RAPID chip.

diameter silicon wafer was cleaned by RCA technique and dehydrated on a hot plate at 120^{o}C for 20 min. SU-8 2005 photoresist was spin-coated on the silicon wafer (500 rpm for 15 sec, followed by 3000 rpm for 30 sec). The resist was soft baked at 90^{o}C for 3 min, followed by UV exposure for 8 sec at 100 mJ/cm^2. Post bake was carried out at 90^{o}C for 1 min and the pattern was developed in SU-8 developer for 4 min. The developed pattern was rinsed in IPA and blow-dried using a nitrogen gun. Finally, a hard bake step was performed at 120^{o}C for 10 min to generate the molding template. The height of the pattern was measured using profilometry.

PDMS base and curing agent were mixed in the ratio of 10:1, degassed and poured on the SU-8 template (master). PDMS was cured by baking it in a hot air oven at 65^{o}C for 45 min. The device was then cut using a surgical blade (no. 12) and gently peeled from the SU-8 master. The two outlets for collecting platelets and RBCs, and the central inlet were punched in the device using a 1.5 mm biopsy punch. The PDMS device was then bonded to a glass cover slip using oxygen plasma for 120 sec. No surface treatment of the PDMS device was performed prior to platelet enrichment experiments.

2.4 Collection of blood and sample preparation

A trained phlebotomist drew 2 ml of blood from healthy volunteers and transferred the blood to an EDTA-coated vacutainer tube. The blood was stored at 4^{o}C in a fridge. It was used within 48 h of collection. Before each cell sorting experiment, the vacutainer tube containing the blood was taken out of the fridge and kept outside for 25 min to allow it to attain room temperature. Sorting experiments were performed with both blood diluted twenty times in normal saline and whole blood. Blood samples were collected from the inlet and each of the two outlets after the

experiment, and taken to the hospital for counting using a hematology analyzer. The level of activation of the platelets after the experiment was also tested.

2.5 Platelet sorting experiment

A 1 ml syringe was filled with whole or dilute blood and mounted on the syringe pump as shown in figure 1(D). The inlet of the chip was connected to the syringe using a 30 cm length of tubing. A vibrator motor was attached to the inlet tubing, at a distance of 15 cm from the chip. The motor was turned on for 40 sec after every 20 min. Inlet flow rates of 600 nl/min, 700 nl/min, 1 μl/min, 3 μl/min, 5 μl/min and 10 μl/min were explored to study the effect of flow rate on the cell sorting parameters in RAPID.

Two separate Eppendorf tubes were used for collecting the platelets and the RBCs. Once 50 μl of sample was collected from the RBC outlet, the tubing connecting the chip to the RBC outlet was clamped. This prevented the blood from flowing to the RBC outlet and increased the sample flow to the platelet outlet. The sorting experiment was over when approximately 25 μl of sample was collected from each of the platelet outlets. The samples from the two platelet outlets were combined for counting. For each flow rate, the number of platelets present in the blood samples from the inlet and the two outlets (RBC and platelet outlets) were counted using a hematology analyzer. Some of the sorting experiments were recorded under an inverted microscope at 25 fps. The frames were extracted from the videos using a MATLAB code and the path of the cells were tracked.

3 Results and discussion

3.1 Device design considerations

The design principle of RAPID has been discussed extensively in an earlier publication[48]. In the first report on RAPID, there were nine, eleven and thirty-nine rows of pillars respectively in the three zones. We saw that ≈ 90% of the particles were trapped efficiently by the first six or seven rows of pillars. Therefore, in the current design, we decided to retain only nine rows in each zone to reduce the device footprint and the sample volume. We retained the circular shape for the pillars as it ensures minimal contact between the pillar and the cells as they pass through the narrow gaps. Also, the cells experience a gradual pressure change while passing through the gaps between circular pillars, unlike the sudden pressure change associated with other pillar shapes. The radial arrangement of pillars in RAPID obviated the need for any flow focusing or sheath flow unlike other device designs. This is because the inlet is located right at the center of the device, which avoids any interaction of the cells with the channel walls.

In the past, we demonstrated the separation of polystyrene beads, which are practically non-deformable. While designing a device for platelet enrichment, we had to consider both the size and the deformability of different blood cells. WBCs range in size from 10 μm to 30 μm, and are much stiffer than RBCs. Therefore, the pillar gap in the WBC capture zone was set at 5μm to stop WBCs from entering the device, while letting RBCs and platelets pass through.

The pillar gap in the AD zone was progressively increased from 5μm to 10 μm. The driving pressure along the radial direction falls approximately as $\sim \frac{1}{r}$, where r is the distance from the inlet (figure S1 in supplementary information). Increasing the pillar gap reduced the hydrodynamic resistance along the radial direction and ensured that the cells moving radially out of the AD zone at least reached the first row of the RBC capture zone.

Finally, the pillar gap of the RBC capture zone was set at 3 μm to stop RBCs, while allowing the platelets to go through. The channel height in this study was kept 5 μm to prevent the biconcave RBCs from flipping on their sides and flowing through gaps much smaller than their diameter. The supplementary movie SV1 shows two RBCs flipping and passing through the 3 μm pillar gap in a device with 10 μm height (our earlier design). In contrast, the RBCs were always oriented flat in the current prototype of RAPID.

3.2 Radial and cross flows in RAPID

RAPID has a self-unclogging feature due to the generation of cross flows, as shown in the supplementary video SV2. Figure 2 shows the paths taken by three different cells inside RAPID at different time points. These snapshots have been acquired from the supplementary video SV2. Initially (A-D), RAPID functions like a dead-end device and the RBCs follow the radial flow. The red track shows one such radial path. Most of these RBCs are stopped by the first row of pillars (with 3 μm pillar gap) of the RBC capture zone. Since the platelets are much smaller than RBCs, they manage to squeeze through the remaining gap even if an RBC is stuck between two pillars. The blue track shows the path of a small cell (possibly platelet) which continues to move radially outwards through the RBC capture zone towards the platelet outlet. Once the radial flow is reduced, a cross flow towards the RBC outlet is automatically set up (E-F), as shown by the green track of an RBC. The angular pillar

arrangement in the AD zone ensures that the cross flow is self-circulating and can carry the larger cells towards the RBC outlet. The supplementary video SV3 shows the steady state operation of the device where the RBCs are continuously carried away by the cross flow. It is the automatic conversion from dead-end to cross flow mode of operation that makes it possible to use RAPID for several hours without clogging, additional buffer injection or reverse flow.

3.3 Handling blood samples in RAPID

We started our experiments using blood diluted with normal saline. However, one of the device development requirements is minimal pre-processing of the sample. Hence, later we tested the operation of RAPID with whole blood from different individuals having up to 50% hematocrit. In this report, we used a syringe pump to drive the flow, so that the optimal flow rate range for platelet enrichment can be accurately determined. We have also operated the device under passive gravity-driven flow (supplementary information). We can use whole blood in RAPID with both pressure-driven and gravity-driven flows for at least 8 h without any clogging. Since the blood was mixed with EDTA, it did not lead to coagulation during the experiment.

When the flow is driven using syringe pump, blood cells tend to settle in the horizontal tube connecting the syringe with the chip

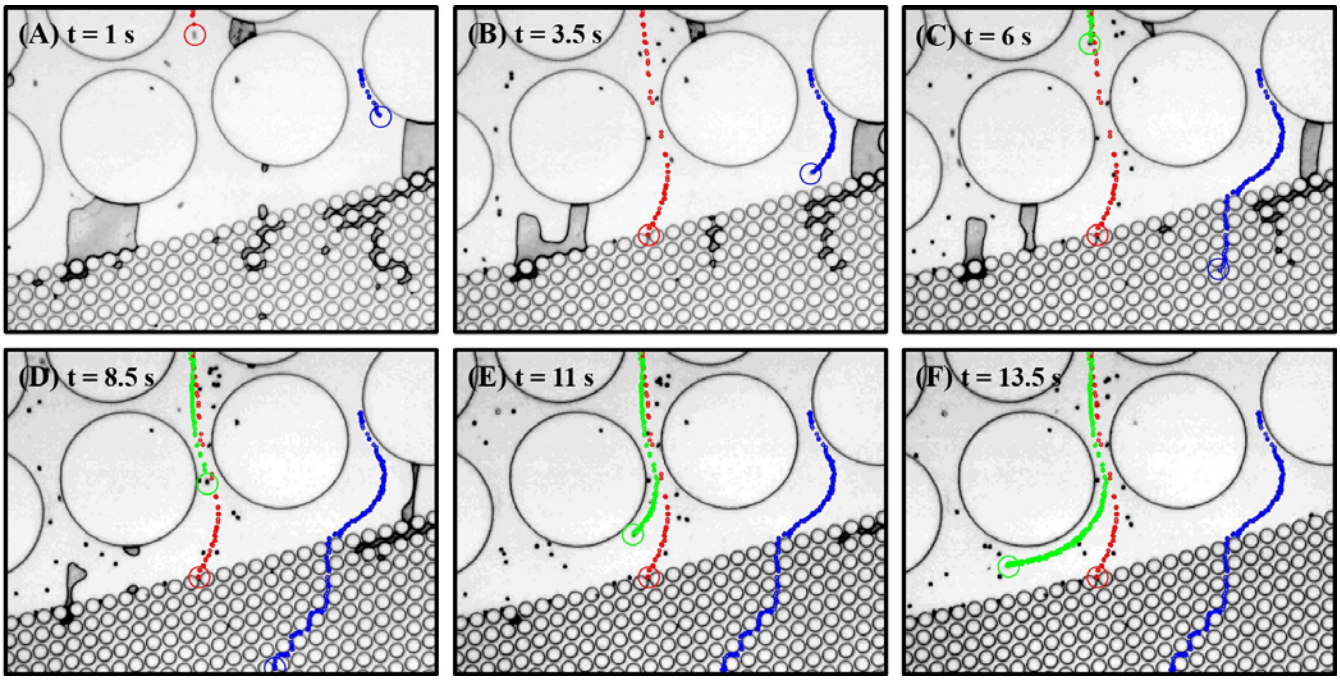

Fig. 2 Time lapse images showing the paths followed by the different cells. At the beginning of the experiment (t=1 s to t = 3.5 s), the RBCs follow a radial path (red track) to reach the RBC capture zone, where they are stopped by the pillars. The smaller cells can still follow a radial path (blue track) towards the platelet outlet. Around t = 8.5 s, many of the radial paths are blocked by the trapped RBCs. This forces the newer RBCs reaching this region to follow the cross flow (green track) towards the RBC outlet.

(supplementary information). This leads to loss of cells during the experiment and adversely affects the recovery parameter. Hence, we attached a vibrator motor at the halfway of the tube between the syringe and the chip. Attaching the motor to the syringe predictably did not have any effect. On the other hand, the vibration was strong enough to dislodge the connectors, if the motor was attached to the tube too close to the chip. Hence, the halfway distance was finally chosen. We observed that a significant number of RBCs settle in the tube in 20 min. We developed a controller circuit (supplementary information) to pre-program the motor to automatically turn it on after every 20 min. The duration of vibration was chosen to be 40 sec by trial and error to re-disperse the blood cells. The circuit for controlling the motor is given in figure S2 of supplementary information.

3.4 Device performance parameters

Platelet enrichment in RAPID was evaluated in terms of purity, enrichment factor, throughput and recovery. Experiments with forty-two different devices were performed with dilute and whole blood at each of the six flow rates (N = 4 for dilute blood, and N =3 for whole blood at

each flow rate) to account for any deviceto-device variability. Different flow rates were explored to find the optimal operating conditions. The samples collected from the two platelet outlets were combined for calculating the separation parameters.

The separation parameters were computed considering only the RBCs and the platelets due to two reasons. First, it was not always possible to use the blood within the first six hours of collection, and as a result, we rarely had viable WBCs in the sample. Second, if there were any WBCs in the sample, they were stopped effectively at the inlet itself due to our device design. The large area (≈1.5mm diameter) of the inlet helped us to avoid any possible clogging of the device as a result of WBCs collecting in the inlet. We also operated the device using simple gravity-driven flow to evaluate its potential for point-of-care applications. The experimental set-up and the device performance parameters are given in figure S3 of supplementary information.

$$Purity = \frac{Number\ of\ platelets}{Total\ number\ of\ RBCs\ and\ platelets} \quad (1)$$

The separation purity of the platelets is defined by equation 1 and is measured at the platelet outlet. The total number of cells at a particular outlet is obtained by adding the number of platelets with the number of RBCs. As shown in figure 3 (A), the separation purity of platelets varies inversely with the inlet flow rate. We achieved ≈ 70% purity at the lowest flow rate of 600 nl/min with both whole and dilute blood.

Platelet enrichment factor =
(Number of platelets at outlet/ Number of RBCs at outlet) /
(Number of platelets at inlet/Number of RBCs at inlet) *(2)*

Figure 3 (B) shows the variation in platelet enrichment factor with flow rate, as defined by equation 2. It is a measure of how well the desired cells (platelets) are concentrated compared to the undesired cells (RBCs) at the two platelet outlets. At the lowest flow rate of 600 nl/min, RAPID can achieve up to 50-fold enrichment of platelets with dilute blood and up to 60-fold enrichment

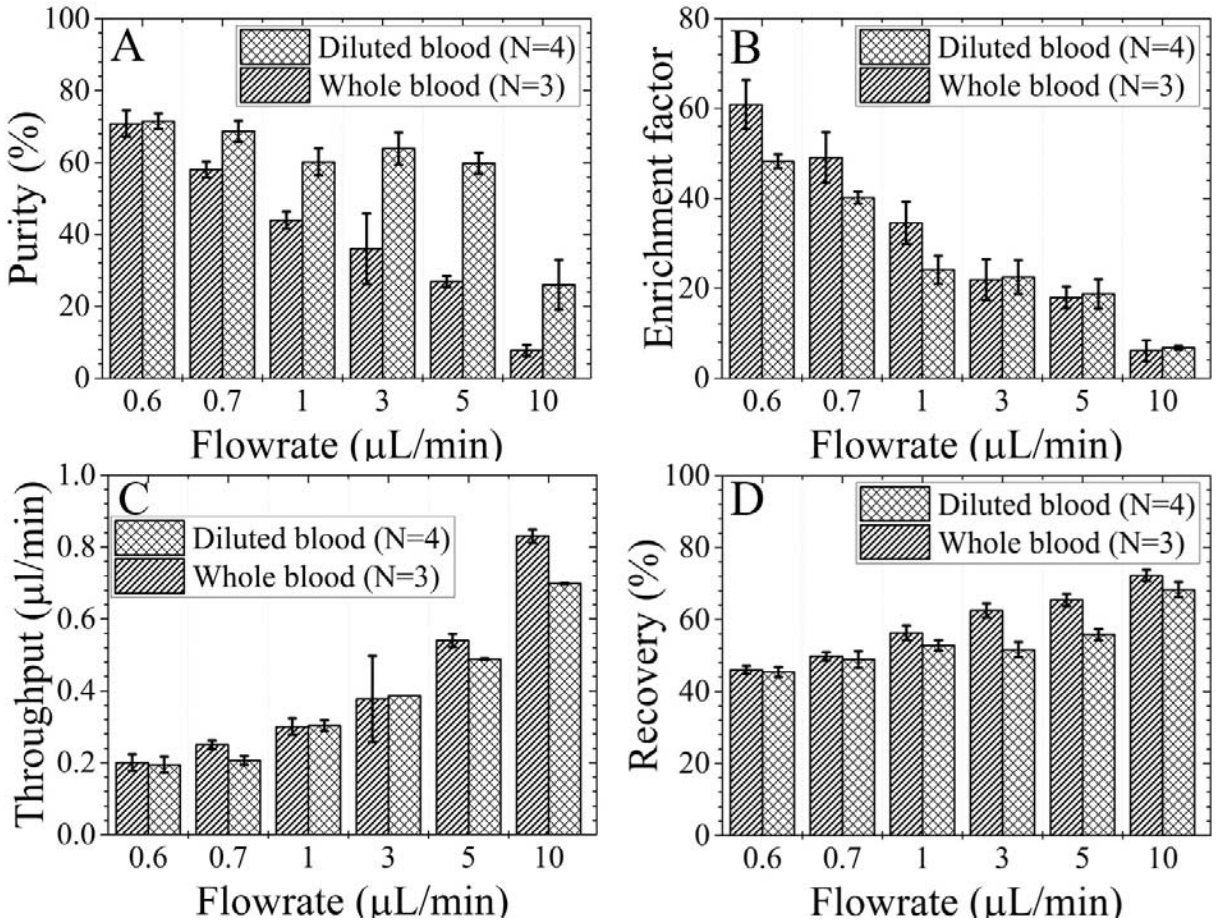

Fig. 3 Platelet separation parameters as a function of flow rate in RAPID. The separation purity (A) of platelets decreases from 75% to 10% with increase in flow rate from 0.6 μl/min to 10 μl/min. The reason for this decrease in purity is that more and more deformable RBCs manage to squeeze through the RBC capture zone towards the platelet outlets with increase in pressure. The platelet enrichment factor (B) also decreases with increase in flow rate due to the same reason.

We can achieve ≈ 50 to 60-fold enrichment at the lowest flow rate. In contrast, the throughput (C) and the recovery (D) of the device increase with increase in flow rate. This is because the clogged cells are also pushed out of the device under higher pressure.

using whole blood. The platelet enrichment factor also decreases with an increase in flow rate.

The throughput (figure 3 (C)) of a particular device measures the sample volume collected from the outlet per minute. The maximum throughput obtained by us during platelet enrichment is ≈ 0.7 - 0.8 μl/min.

Recovery = *Total number of cells at outlet/ Total number of cells at inlet* **(3)**

The parameter recovery gives us a measure of the number of cells lost in the chip and is given by equation 3. As shown in figure 3(D), platelet recovery increases with the inlet flow rate and varies between 40% to 80% at the flow rates studied.

We find that there is a trade-off between the inlet flow rate and the different device performance parameters. Separation purity and enrichment are the highest at the lower flow rates, while both throughput and recovery increase with an increase in the inlet flow rate. This is because RBCs are very deformable and at higher flow rates RBCs are forced radially outwards through the pillar gaps. As shown in figure 3, the device performance does not change significantly when we replace 20 times diluted blood with whole blood. The purity, throughput and recovery values remain very similar, while platelet enrichment is somewhat more effective with whole blood. This is because there are more RBCs in the whole blood at the inlet, which leads to a higher enrichment value as defined by equation 2. The optimal flow rate for platelet enrichment in RAPID will need to be chosen based on optimal performance parameters and on also the sample under consideration. Platelets get activated at pressures of 10 kPa and above[49]. Therefore, it is desirable to work with low flow rates when handling blood samples. In our study, we have used a maximum inlet flow rate of 10 μl/min, which corresponds to a pressure of 2 kPa (COMSOL simulation, data not shown). We also used the platelet activation function of the hematology analyzer (using the proprietary kit Plachek) during counting to verify that platelets were not activated after passage through RAPID.

Most of the recent reports on microfluidic platelet separation employed an off-chip sample preparation technique, and did not use whole blood. Nam and others[11] worked with whole blood to achieve 98% purity, 74% recovery and 10-fold platelet enrichment. Their device throughput was 250 nl/min. This report used a SAW-based active separation technique, which requires the integration of transducers and the use of high voltages. Our device can work with whole blood (i.e. without any pre-processing) and relies on an entirely passive separation technique. Ours is the first report of a passive pillar-based device which continues to function with whole blood in excess of 8 hours without clogging under both gravity-driven and pressure-driven flows. Based on the various performance parameters, our device can be used for platelet enrichment at flow rates between 600nl/min and 1 μl/min with ≈ 60% purity, ≈ 50% recovery, ≈ 50-fold enrichment and a throughput of 250 nl/min.

4 Conclusions

We demonstrate platelet enrichment from whole blood in a microfluidic radial pillar device (RAPID) recently reported by us. RAPID combines the advantages of both dead-end and cross flow pillar filters. The device starts working like a dead-end pillar filter and automatically converts itself into a cross flow filter at the first signs of clogging. We operated this device with both diluted and whole blood, using pressure-driven and gravity-driven flows. Unlike most reported pillar-based devices, this device could function continuously for more than 8 h without clogging when used with whole blood. We observed that the recovery of platelets and throughput of the device increase with flow rate, while the separation purity and enrichment factor peak at the lowest flow rates. Based on these performance parameters and to avoid platelet activation, we recommend operating RAPID at flow rates between 600nl/min and 1 μl/min to achieve ≈ 50-fold platelet enrichment. We tested RAPID under gravity-driven flow to explore the potential of the device at the point of care, without any external power source. We believe RAPID can be used to develop handheld platelet counters.

Acknowledgements

We would like to thank the Ministry of Electronics and Information Technology (MeitY), Govt. of India, for funding through the Centre for Nanoelectronics (phase 2). The lithography has been performed in the cleanroom of the IIT Bombay Nanofabrication Facility. We would also like to thank Kaushalya Foundation Medical Trust Hospital for technical support and discussions.

References

1 H. Song, H.-W. Li, M. S. Munson, T. G. Van Ha and R. F. Ismagilov, *Analytical chemistry*, 2006, **78**, 4839–4849.

2 S. Kalayanarooj, D. Vaughn, S. Nimmannitya, S. Green,
S. Suntayakorn, N. Kunentrasai, W. Viramitrachai, S. Ratanachu-Eke, S. Kiatpolpoj, B. Innis *et al.*, *Journal of Infectious Diseases*, 1997, **176**, 313–321.

3 A. Regev, P. Stark, D. Blickstein and M. Lahav, *American journal of hematology*, 1997, **56**, 168–172.

4 B. M. Sibai, *Obstetrics & Gynecology*, 2004, **103**, 981–991.

5 N. Nivedita and I. Papautsky, *Biomicrofluidics*, 2013, **7**, 054101.

6 L. Leonard, *Microfluidic blood sample separations*, 2002, US Patent App. 10/205,796.

7 G. Brecher and E. P. Cronkite, *Journal of Applied Physiology*, 1950, **3**, 365–377.

8 V. Rasi, *Thrombosis research*, 1979, **15**, 543–552.

9 J. P. Blass, S. Cederbaum and R. Kark, *Clinica Chimica Acta*, 1977, **75**, 21–30.

10 J. F. Morrow, H. G. Braine, T. S. Kickler, P. M. Ness, J. D. Dick and A. K. Fuller, *Jama*, 1991, **266**, 555–558.

11 J. Nam, H. Lim, D. Kim and S. Shin, *Lab on a Chip*, 2011, **11**, 3361–3364.

12 M. S. Pommer, Y. Zhang, N. Keerthi, D. Chen, J. A. Thomson, C. D. Meinhart and H. T. Soh, *Electrophoresis*, 2008, **29**, 1213–1218.

13 T. K. Tie, M. A. Holmes and A. W. Rank, *Centrifugal separation of blood*, 1989, US Patent 4,850,995.

14 R. Gorkin, J. Park, J. Siegrist, M. Amasia, B. S. Lee, J.-M. Park, J. Kim, H. Kim, M. Madou and Y.-K. Cho, *Lab on a Chip*, 2010, **10**, 1758–1773.

15 M. Amasia and M. Madou, *Bioanalysis*, 2010, **2**, 1701–1710.

16 F. Petersson, L. Åberg, A.-M. Swärd-Nilsson and T. Laurell, *Analytical chemistry*, 2007, **79**, 5117–5123.

17 D. Di Carlo, D. Irimia, R. G. Tompkins and M. Toner, *Proceedings of the National Academy of Sciences*, 2007, **104**, 18892– 18897.

18 A. J. Mach and D. Di Carlo, *Biotechnology and bioengineering*, 2010, **107**, 302–311.

19 D. Di Carlo, J. F. Edd, D. Irimia, R. G. Tompkins and M. Toner, *Analytical chemistry*, 2008, **80**, 2204–2211.

20 A. A. S. Bhagat, H. W. Hou, L. D. Li, C. T. Lim and J. Han, *Lab on a Chip*, 2011, **11**, 1870–1878.

21 M. Yamada, M. Nakashima and M. Seki, *Analytical chemistry*, 2004, **76**, 5465–5471.

22 J. Takagi, M. Yamada, M. Yasuda and M. Seki, *Lab on a Chip*, 2005, **5**, 778–784.

23 M. Toner and D. Irimia, *Annual review of biomedical engineering*, 2005, **7**, 77.

24 D. R. Gossett, W. M. Weaver, A. J. Mach, S. C. Hur, H. T. K. Tse, W. Lee, H. Amini and D. Di Carlo, *Analytical and bioanalytical chemistry*, 2010, **397**, 3249–3267.

25 T. Geislinger, B. Eggart, S. Braunmüller, L. Schmid and T. Franke, *Applied Physics Letters*, 2012, **100**, 183701.

26 L. R. Huang, E. C. Cox, R. H. Austin and J. C. Sturm, *Science*, 2004, **304**, 987–990.

27 S. H. Holm, J. P. Beech, M. P. Barrett and J. O. Tegenfeldt, *Lab on a Chip*, 2011, **11**, 1326–1332.

28 S. Zheng, R. Yung, Y.-C. Tai and H. Kasdan, 18th IEEE International Conference on Micro Electro Mechanical Systems, 2005. MEMS 2005., 2005, pp. 851–854.

29 J. A. Davis, D. W. Inglis, K. J. Morton, D. A. Lawrence, L. R. Huang, S. Y. Chou, J. C. Sturm and R. H. Austin, *Proceedings of the National Academy of Sciences*, 2006, **103**, 14779–14784.

30 N. Li, D. T. Kamei and C.-M. Ho, 2007 2nd IEEE International Conference on Nano/Micro Engineered and Molecular Systems, 2007, pp. 932–936.

31 S. Choi, S. Song, C. Choi and J.-K. Park, *Lab on a Chip*, 2007, **7**, 1532–1538.

32 H. M. Ji, V. Samper, Y. Chen, C. K. Heng, T. M. Lim and L. Yobas, *Biomedical microdevices*, 2008, **10**, 251–257.

33 A. A. S. Bhagat, H. Bow, H. W. Hou, S. J. Tan, J. Han and C. T. Lim, *Medical & biological engineering & computing*, 2010, **48**, 999–1014.

34 V. VanDelinder and A. Groisman, *Analytical chemistry*, 2006, **78**, 3765–3771.

35 V. VanDelinder and A. Groisman, *Analytical Chemistry*, 2007, **79**, 2023–2030.

36 X. Chen, C. C. Liu, H. Li *et al.*, *Sensors and Actuators B: Chemical*, 2008, **130**, 216–221.

37 C. W. Shields IV, C. D. Reyes and G. P. López, *Lab on a Chip*, 2015, **15**, 1230–1249.

38 J. El-Ali, P. K. Sorger and K. F. Jensen, *Nature*, 2006, **442**, 403–411.

39 M. M. Wang, E. Tu, D. E. Raymond, J. M. Yang, H. Zhang, N. Hagen, B. Dees, E. M. Mercer, A. H. Forster, I. Kariv *et al.*, *Nature biotechnology*, 2005, **23**, 83–87.

40 H. Andersson and A. Van den Berg, *Sensors and Actuators B: Chemical*, 2003, **92**, 315–325.

41 J. Nam, H. Lim, D. Kim, H. Jung and S. Shin, *Lab on a chip*, 2012, **12**, 1347–1354.

42 Y. Chen, M. Wu, L. Ren, J. Liu, P. H. Whitley, L. Wang and T. J. Huang, *Lab on a Chip*, 2016, **16**, 3466–3472.

43 H. Xia, B. C. Strachan, S. C. Gifford and S. S. Shevkoplyas, *Scientific Reports*, 2016, **6**, 35943.

44 L. Basabe-Desmonts, S. Ramstrom, G. Meade, S. OâA˘Zneill,´ A. Riaz, L. Lee, A. Ricco and D. Kenny, *Langmuir*, 2010, **26**, 14700–14706.

45 H. W. Hou, A. A. S. Bhagat, W. C. Lee, S. Huang, J. Han and C. T. Lim, *Micromachines*, 2011, **2**, 319–343.

46 S. Yang, A. Ündar and J. D. Zahn, *Lab on a Chip*, 2006, **6**, 871–880.

47 S. M. McFaul, B. K. Lin and H. Ma, *Lab on a chip*, 2012, **12**, 2369–2376.

48 N. Mehendale, O. Sharma, C. Dcosta and D. Paul, MicroTAS 2016, 2016.

49 E. Gutierrez, B. G. Petrich, S. J. Shattil, M. H. Ginsberg, A. Groisman and A. Kasirer-Friede, *Lab on a Chip*, 2008, **8**, 1486–1495.